

# Lawrence Berkeley National Laboratory

## Recent Work

**Title**

MERLIN - A meV resolution beamline at the ALS

**Permalink**

<https://escholarship.org/uc/item/0jq9494w>

**Journal**

AIP Conference Proceedings, 879(1)

**ISSN**

0094-243X

**ISBN**

9780735403734

**Authors**

Reininger, R  
Bozek, J  
Chuang, YD  
[et al.](#)

**Publication Date**

2007-03-26

**DOI**

10.1063/1.2436110

Peer reviewed

# MERLIN — A meV Resolution Beamline at the ALS

Cite as: AIP Conference Proceedings **879**, 509 (2007); <https://doi.org/10.1063/1.2436110>  
Published Online: 07 February 2007

Ruben Reininger, John Bozek, Yi-De Chuang, Malcolm Howells, Nicholas Kelez, Soren Prestemon, Steve Marks, Tony Warwick, Chris Jozwiak, Alessandra Lanzara, M. Zahid Hasan, and Zahid Hussain



View Online



Export Citation

## ARTICLES YOU MAY BE INTERESTED IN

[Invited Article: High resolution angle resolved photoemission with tabletop 11 eV laser](#)  
Review of Scientific Instruments **87**, 011301 (2016); <https://doi.org/10.1063/1.4939759>

[High-efficiency in situ resonant inelastic x-ray scattering \(iRIXS\) endstation at the Advanced Light Source](#)

Review of Scientific Instruments **88**, 033106 (2017); <https://doi.org/10.1063/1.4977592>

[A facility for the analysis of the electronic structures of solids and their surfaces by synchrotron radiation photoelectron spectroscopy](#)

Review of Scientific Instruments **88**, 013106 (2017); <https://doi.org/10.1063/1.4973562>

## Lock-in Amplifiers up to 600 MHz

starting at

\$6,210



Zurich  
Instruments

Watch the Video



# MERLIN - A meV Resolution Beamline at the ALS

Ruben Reininger<sup>1</sup>, John Bozek<sup>2</sup>, Yi-De Chuang<sup>2</sup>, Malcolm Howells<sup>2</sup>, Nicholas Kelez<sup>2</sup>, Soren Prestemon<sup>2</sup>, Steve Marks<sup>2</sup>, Tony Warwick<sup>2</sup>, Chris Jozwiak<sup>2,3</sup>,  
Alessandra Lanzara<sup>2,3</sup>, M. Zahid Hasan<sup>2,4</sup>, Zahid Hussain<sup>2</sup>

<sup>1</sup>*Scientific Answers & Solutions, 5708 Restal St., Madison, WI 53711, USA*

<sup>2</sup>*Advanced Light Source, Lawrence Berkeley National Laboratory, CA 94720, USA*

<sup>3</sup>*University of California at Berkeley, CA 94720, USA*

<sup>4</sup>*Joseph Henry Laboratories, Department of Physics, Princeton University, Princeton, NJ 08544, USA*

**Abstract.** An ultra-high resolution beamline is being constructed at the Advanced Light Source (ALS) for the study of low energy excitations in strongly correlated systems with the use of high-resolution inelastic scattering and angle-resolved photoemission. This new beamline, given the acronym Merlin (for meV resolution line), will cover the energy range 10-150 eV. The monochromator has fixed entrance and exit slits and a plane mirror that can illuminate a spherical grating at the required angle of incidence (as in the SX-700 mechanism). The monochromator can be operated in two different modes. In the highest resolution mode, the energy scanning requires translating the monochromator chamber (total travel 1.1 m) as well as rotating the grating and the plane mirror in front of the grating. The resolution in this mode is practically determined by the slits width. In the second mode, the scanning requires rotating the grating and the plane mirror. This mode can be used to scan a few eV without a significant resolution loss. The source for the beamline is a 1.9 m long, 90 mm period quasi periodic EPU. The expected flux at the sample is higher than  $10^{11}$  photons/s at a resolving power of  $5 \times 10^4$  in the energy range 16-130 eV. A second set of gratings can be used to obtain higher flux at the expense of resolution.

**Keywords:** Monochromator, EUV, EPU, beamline, ALS.

**PACS:** 07.85.Qe, 41.60.-m, 42.79.Dj

## INTRODUCTION

The MERLIN beamline is part of an ALS program dedicated to the study of complex systems. The photon source is a state of the art quasi-periodic elliptically polarizing undulator designed to suppress higher order radiation at the sample. The experimental equipment includes a station with a high resolution/throughput spectrograph [1] suitable for carrying out inelastic scattering studies of strongly correlated systems and a system for angle-resolved photoemission spectroscopy (ARPES).

The experimental requirements are a resolution better than 1 meV in the energy range between 8 and 100 eV. This range, which is beyond that of normal incidence instruments, and the requirement for fixed entrance and exit slits, led us to implement a monochromator operating on the Rowland circle when ultimate resolution is required. The adopted design allows for a second, and simpler, mode of operation in which a few eV can be scanned with a stationary grating chamber without a severe penalty in resolution. The beamline and the insertion device are being constructed. They are expected to become operational in July 2007.

## MONOCHROMATOR

The monochromator chosen for the MERLIN beamline is a quasi-Rowland circle instrument with fixed entrance and exit slits similar to those described by Ishiguro *et al.* [2] and by Senf *et al.* [3]. In its basic configuration, [2, 3] a plane mirror at a fixed angle of incidence is used together with the grating to keep the incident and diffracted beams parallel. The energy scanning is performed by rotating the grating and translating the two elements along the incident beam. This mode of operation focuses at one photon energy, where it fulfills the Rowland condition i.e.,

CP879, *Synchrotron Radiation Instrumentation: Ninth International Conference*,

edited by Jae-Young Choi and Seungyu Rah

© 2007 American Institute of Physics 978-0-7354-0373-4/07/\$23.00

$r_1 = R \cos \alpha$  and  $r_2 = R \cos \beta$ . In the previous equations,  $R$  is the grating radius,  $r_1$  and  $r_2$  the entrance and exit slit distances to the grating,  $\alpha$  is the angle of incidence and  $\beta$  is the diffraction angle. As Senf *et al.*[3] pointed out, the monochromator can fulfill the Rowland condition by varying the angle of incidence on the plane mirror.

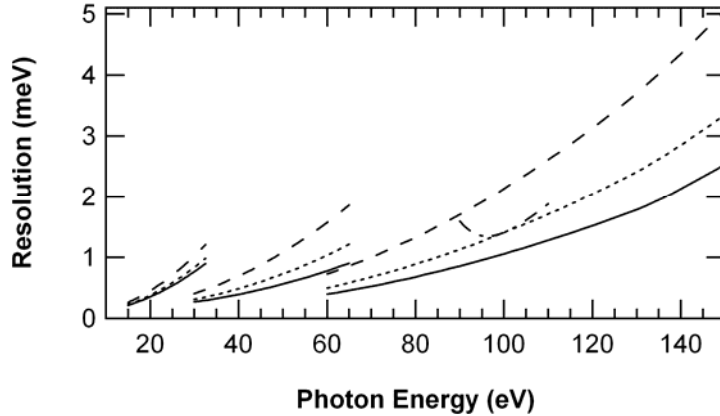


**FIGURE 1.** Total resolution expected with the three HR gratings. Solid lines: No SE on the plane mirror and gratings; Dotted lines: RMS SE of 0.25  $\mu\text{rad}$ ; Dashed lines: RMS SE of 0.5  $\mu\text{rad}$ . Dot-dashed lines: fixed grating chamber (see text). The slits width is set to 10  $\mu\text{m}$  for the LEG and 5  $\mu\text{m}$  for the MEG and HEG.

In the present instrument, the SX-700 mechanism [4] implemented in a beamline at the ALS [5] is used to vary the angle of incidence on the plane mirror. The monochromator length is 7.7 m and the total translation of the plane mirror-grating chamber (PMGC) is 1.1 m.

In the high-resolution (HR) mode of operation, the PMGC position and the angles on the mirror and grating are determined by the Rowland condition and the grating equation. This mode employs three gratings having line densities of 900 (LEG), 1800 (MEG), and 3600 (HEG) 1/mm to achieve a resolving powers higher than  $5 \times 10^4$  between 15 and 130 eV. The three gratings are in a single substrate with  $R=15$  m. The angle of incidence on the plane mirror required to scan this energy range varies between  $74.95^\circ$  and  $75.08^\circ$ . Figure 1 shows the total resolution expected in this mode without slope errors (SE) on the plane mirror and on the grating and with RMS SE of 0.25 and 0.5  $\mu\text{rad}$  on these elements. In addition to the slope errors, the calculations include the contributions due to 10  $\mu\text{m}$  slits for the LEG and 5  $\mu\text{m}$  for the MEG and HEG, spherical aberration, and line curvature.

The SX-700 mechanism allows scanning a few eV with high resolution without translating the PMGC. This is shown by the dot-dashed line in Fig. 1. In this example, the PMGC was positioned for optimum resolution at 100 eV and the scanning is performed by varying the included angle such that at each photon energy the overall contribution to the resolution due to the defocus, coma, and spherical aberration is minimized.

A second set of gratings having line densities of 300 (LEG), 600 (MEG), and 1200 (HEG) 1/mm is used in the high flux (HF) mode. These gratings are in a single substrate with  $R=18.6$  m. The Rowland condition is fulfilled with the LEG (MEG, HEG) between 8 and 16.5 eV (16-33 eV, 32-66 eV). However, the freedom of varying the included angle to minimize the sum of the aberrations yields good resolution in a wider energy range for each grating.

## PRE AND POST FOCUSING OPTICS

A cartoon drawing of the beamline showing its main components and the two experimental stations is presented in Fig. 2. The first optical component, located inside the ring shielding, is a spherical mirror that deflects the beam horizontally by  $2.5^\circ$  and focuses along the horizontal direction at the exit slit with a magnification of 1.3. The next element is a sagittal cylinder deflecting the beam horizontally by  $13^\circ$ . This element demagnifies the source along the vertical (dispersion) direction by a factor of 5.1 at the entrance slit. Both mirrors are coated with graphite and internally water-cooled to prevent heat-load induced deformations that could impair the beamline performance. The monochromator is seen at the center of Fig. 2. The plane mirror and the grating are also internally water-cooled.

One of the two interchangeable plane mirrors downstream the exit slit deflects the beam horizontally by  $10^\circ$  ( $23.5^\circ$ ) towards the RIXS (ARPES) experimental station. The imaging of the exit slit onto each station is done with a sagittally-focusing cylinder followed by a plane mirror bent into an elliptical cylinder. Each mirror deflects the beam

vertically by  $14^\circ$ . The cylinder demagnifies horizontally onto the RIXS (ARPES) station by a factor of 3.2 (2.8) whereas the elliptical cylinder demagnifies vertically onto the RIXS (ARPES) by 5.5 (4.8).

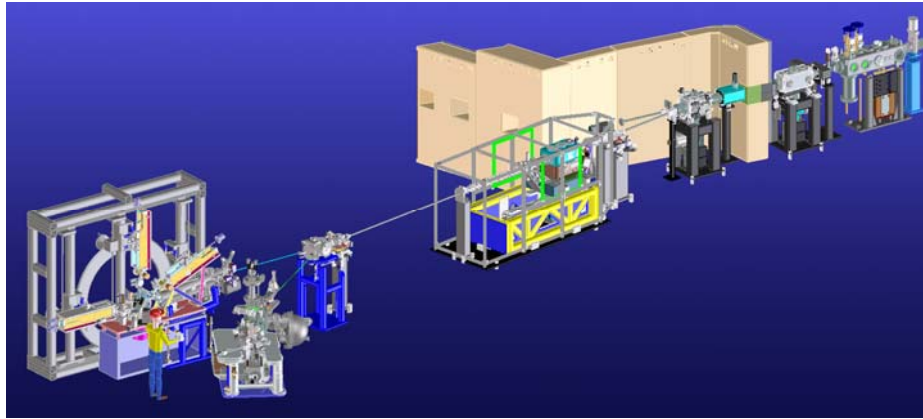


**FIGURE 2.** CAD drawing of the MERLIN beamline and the two experimental stations

## RAY TRACINGS

To verify the analytical results for the resolution, several ray tracings were performed using SHADOW [6] at different energies for each grating. As described above, the source is focused at the entrance slit only along the vertical direction whereas along the horizontal direction it is focused at the exit slit. To include the diffraction at the exit slit, two sets of ray tracings were performed. In the former set, up to the entrance slit, the beam sizes and divergences were calculated from the vector sum of the electron RMS values and the photon values,  $\sigma_p$ , and  $\sigma_r$ . These were calculated using the approximations  $\sigma_p = \sqrt{\lambda/2L}$  and  $\sigma_r = \sqrt{2\lambda L}/(4\pi)$ , where  $\lambda$  is the wavelength and  $L$  the length of the insertion device. The second set of ray traces was performed from the entrance slit plane up to the sample. For the horizontal size and divergence, the values obtained from the ray traces at the entrance slit plane were used. In the cases where diffraction at the slit dominated the vertical divergence, we used a Gaussian distribution with a RMS value equal to  $0.37 \lambda/s$ . Otherwise, the results obtained at the entrance slit were used as the source.

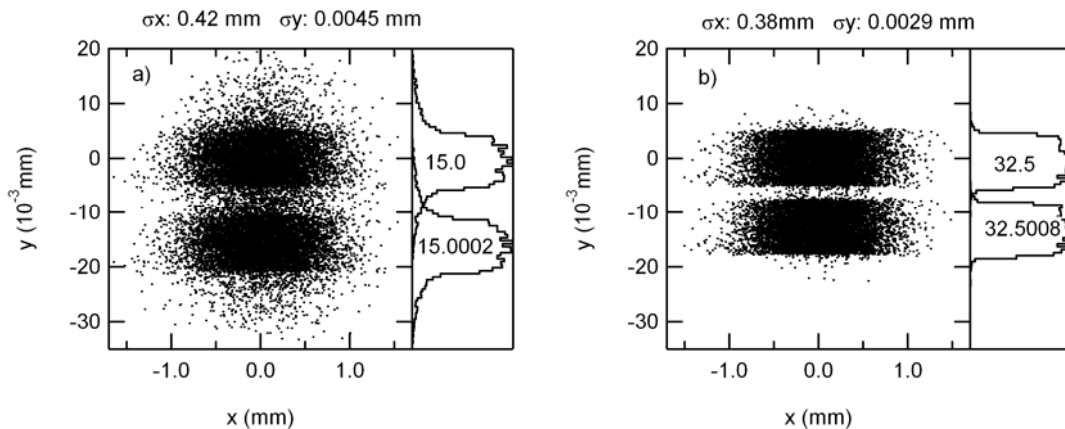


**FIGURE 3.** Spot patterns at the exit slit with the HR LEG. a) 15.0 and 15.0002 eV; b) 32.5 and 32.5008 eV. The slits width is  $10 \mu\text{m}$ . The RMS values of the beam size at the central energy are given in each figure.

Figure 3 shows an example of the spot patterns at the exit slit plane obtained with the HR LEG at the minimum and maximum energies of its range. No slope errors were assumed on the optics. The ray tracings at the second energy shown in each figure were obtained with the same monochromator settings as the central energy. As seen in each figure, there is no visible coma. The symmetric “tail” observed at the lowest energy (Fig. 3a) is mainly due to spherical aberration induced by the large diffraction at the slit. This contribution is significantly less at 32.5 eV (Fig. 3b) since the diffraction is here smaller. The separation between the two energies indicates that the resolving power

is better than 75000 at 15 eV and better than 40000 at 32.5 eV. Including a contribution of a 10  $\mu\text{m}$  slit yield very similar values to those reported in Fig. 1.

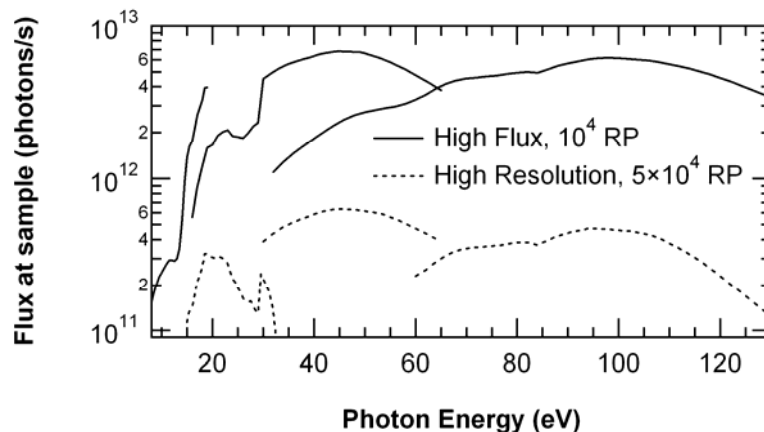


**FIGURE 4.** Flux expected at the RIXS station at a resolving power of  $5 \times 10^4$  with the three HR (dotted lines) and of  $10^4$  with the three HF (solid lines) gratings.

## FLUX

The source for the MERLIN beamline is a quasi-periodic [7] elliptical polarized undulator (QPEPU) that delivers horizontal, vertical, and circular polarized radiation in the beamline range. The ID has 19 periods of 90 mm each.

The flux at the sample position was calculated for resolving powers of  $5 \times 10^4$  with the HR gratings and  $10^4$  with the HF gratings. The following factors were taken into account: i) The flux emitted in  $0.9 \times 0.9 \text{ mrad}^2$  by the ID when set for horizontally polarized radiation ii) The reflectivities of all mirrors, iii) The grating efficiencies, and iv) The transmission of the entrance slit when set to obtain the corresponding resolving power.

The reflectivities of all the mirrors were calculated for energies larger than 30 eV using the atomic scattering factors from Henke *et al.* [8] Below 30 eV the data compiled by Palik [9] was used. The grating efficiencies were calculated using the differential formalism of the exact electromagnetic theory [10] with optimized trapezoidal gratings. For the HR gratings the efficiency varies between 8 and 24 %, for the HF gratings between 15 and 31%.

The calculated flux at the sample position for the HR and HF gratings is displayed in Fig. 4. More than  $10^{11}$  photons/sec are expected at a RP of  $5 \times 10^4$  from 16 up to 130 eV. The flux with the HF gratings with the slits tuned to deliver  $10^4$  resolving power is almost one order of magnitude higher.

## ACKNOWLEDGMENTS

The Advanced Light Source and the MERLIN project are funded by the Office of Basic Energy Sciences (BES), U.S. Department of Energy (DOE) with contract DE-AC03-76SF00098 at LBNL.

## REFERENCES

1. Yi-De Chuang, J. Pepper, W. McKinney, Z. Hussain, E. Gullikson, P. Batson, D. Qian, and M.Z. Hasan, *J. Phys. Chem. Solids*, **66**, 2173-2178, 2005
2. E. Ishiguro, M. Suzui, J. Yamazaki, E. Nakamura, K. Sakai, O. Matsudo, N. Mizutani, K. Fukui, and M. Watanabe, *Rev. Sci. Instrum.*, **60**, 2105, 1989
3. F. Senf, F. Eggenstein, and W. Peatman, *Rev. Sci. Instrum.*, **63**, 1326, 1992
4. F. Riemer and R. Torge, *Nucl. Instr. Methods*, **208**, 313, 1983
5. T. Warwick, N. Andresen, J. Comins, L.K. Kaznatcheyev, J.B. Kortright, J.P. McKean, H.A. Padmore, D.K. Shuh, T. Stevens, and T. Tyliszczak, *AIP Conf. Proc.*, **705**, 458-461, 2004
6. C. Welnak, G.J. Chen, and F. Cerrina, *Nucl. Instr. Methods A*, **347**, 344, 1994
7. S. Sasaki, H. Kobayashi, M. Takao, Y. Miyahara, and S. Hashimoto, *Rev. Sci. Instrum.*, **66**, 1953, 1995
8. B.L. Henke, E.M. Gullikson, and J.C. Davis, *Atomic Data and Nuclear Tables*, **54**, 181-342, 1993
9. E. Palik, ed. *Handbook of Optical Constants of Solids*. Handbook of Optical Constants of Solids. Vol. II. 1991, Academic Press: New York.
10. M. Neviere, P. Vincent, and R. Petit, *Nouv. Rev. Optique*, **5**, 65, 1974